On the influence of solute polarizability on the hydrophobic interaction

Fernando Bresme[a] and Aaron Wynveen[b]
Department of Chemistry, Imperial College London, Exhibition Road, London SW7 2AZ, United Kingdom

(Received 25 September 2006; accepted 6 December 2006; published online 23 January 2007)

The authors have performed molecular dynamics simulations of polarizable solutes in water to investigate how solute polarizability affects solute-solute hydrophophic interactions. A degree of polarization similar to the one expected in biomolecules, corresponding to a dielectric response of $\epsilon=2-20$, results in dramatic changes in the hydrophobic forces. They find that this degree of polarizability is enough to inhibit drying between hydrophobic solutes and to stabilize a reduced water density phase whose density is smaller than the bulk water density. The hydrophobic forces associated with such reduced density states are still very significant with values of the order of several tens of piconewtons. Their results suggest that polarizability plays an important role in determining the hydrophobic force acting between weakly polar surfaces. © *2007 American Institute of Physics*. [DOI: 10.1063/1.2431167]

I. INTRODUCTION

The hydrophobic interaction is considered to be one of the main driving forces acting in the self-assembly of surfactants into micelles and bilayers,[1] and it has been advocated as one of the main contributions to the forces regulating protein folding.[2] Water near hydrophobic surfaces exhibits a complex behavior. New insights into this behavior, both in material and biological interfaces, have been obtained through vibrational sum frequency and femtosecond laser spectroscopy experiments.[3,4] On theoretical grounds, Stillinger[5] suggested that the water hydrogen-bond structure around hydrophobic solutes is modified with respect to the bulk and depends on the solute curvature. These modifications can be used to explain the peculiar thermodynamic behavior associated with hydrophobicity,[6,7] such as the large change in the heat capacity associated with the solvation of hydrocarbons in water. Similar changes are also observed in protein folding, a fact that emphasizes the importance of hydrophobic interactions in these biological processes.[8] Despite the number of works devoted to understand the origin of the hydrophobic interaction, there is still a need to understand the microscopic mechanism behind this interaction as well as the exact role played by water in the self-assembly of hydrophobic objects.

Several experiments have reported strong long-range forces between hydrophobic surfaces,[9] which could not be explained in terms of van der Waals interactions alone. They were thought to originate from the formation of small bubbles bridging the hydrophobic surfaces; a notion that supports drying between hydrophobic objects as a mechanism for self-assembly at the molecular scale. This idea has been summarized in a general theory of solvation by Lum *et al.*[10] The exact mechanism for the hydrophobic interaction, however, remains a matter of dispute. The rationale behind the formation of bubbles, i.e., cavitation, is far from clear.[11] Estimates of the free energy of cavity formation suggest that cavitation may not be kinetically favored at ambient temperatures.[12] Furthermore, surface force apparatus experiments have reported cavitation only at or close to surface contact,[11] and recent computer simulations suggest that cavitation is rather sensitive to the interactions between the solvent and the hydrophobic surfaces.[13,14] Moreover, a recent neutron reflectivity experiment has reported a fluctuating reduced water density region between hydrophobic surfaces,[15] suggesting the absence of drying between hydrophobic objects.

Regarding biological processes such as protein folding, nuclear magnetic resonance experiments demonstrate that water can still be found inside proteins upon folding,[16] an observation consistent with recent computer simulations of proteins.[17,18] Furthermore, results of contrasting protein computer simulations[17,19] suggest that drying inside proteins is very sensitive to protein-water interactions and that, as a matter of fact, the hydrophobic regions in biomolecules are not purely hydrophobic. Both experiments and simulations indicate that hydrophobic regions in proteins are actually polar to a certain extent, with permittivities ranging from $\epsilon \sim 4$,[16] for hydrophobic spots, to $\epsilon \sim 10$,[20] for regions of catalytic importance.

Most studies of hydrophobic interactions to date have not explicitly incorporated the polarizability of the hydrophobic solute. Nevertheless, there are some exceptions in which polarization and its possible effects have been considered, specifically for the case of the passage of water through microscopically narrow channels.[21] This study has highlighted the importance of taking into account the polarizability of the media to adequately characterize such confined systems, an idea advanced by Parsegian[22] many years ago for biological channels.

Our primary objective in this work lies in determining the effect of solute polarizability, a realistic property of hy-

[a]Electronic mail: f.bresme@imperial.ac.uk
[b]Electronic mail: a.wynveen@imperial.ac.uk

drophobic materials, on solute-solute interactions mediated by water and quantifying the level of solute polarizability that is needed to inhibit drying.

II. MODEL AND SIMULATION DETAILS

We have focused our investigations on hydrophobic objects with a simple cylindrical geometry of radius $R \approx 8.5$ Å. A solute of this shape and size is relevant for models of protein bundles or DNA,[23] as well as nanorod materials. Similar models have also been considered in theoretical treatments based on the square gradient theory.[10] In the present paper the explicit treatment of the solute polarizability is handled through an induced surface charge approach,[24] where each charge outside the polarizable solute generates a surface charge on the solute. The induced surface charge distribution depends on the magnitude and location of the external charges as well as on the dielectric permittivity of the solute. We treat the solute as an isotropic linear dielectric so that its degree of polarizability is quantified by an effective dielectric constant ϵ_{in}. Water is included explicitly in our simulation through the simple point charge extended[25] (SPC/E) water model. This water model is comparable in accuracy, with regard to the water bulk properties at ambient temperatures, to more complex water models.[26] Also, it has been shown that the simulations of SPC/E water next to surfaces with markedly different polarizabilities (hydrophobic and metallic) render essentially the same results regarding the water structure and the associated electrostatic fields.[27,28]

The method used to model polarizable solutes is detailed in Ref. 24. Beginning with the potential due to an external point charge in free space given by Poisson's equation for a charge q,[29]

$$\nabla^2 \psi(\mathbf{r}) = -\frac{q}{\epsilon_0}\delta(\mathbf{r}-\mathbf{r}'), \tag{1}$$

we use the boundary conditions that the potential and the normal component of the displacement field across the solute surface must be continuous to determine the potential in all regions of space (inside and outside the dielectric solute). Upon calculation of this potential, the induced charge on the surface of the solute may be calculated, assuming a sharp dielectric discontinuity at the solute surface, and it is given by

$$\sigma_{\text{ind}}(\mathbf{r}_{\text{surf}}) = \mathbf{P}\cdot\hat{n} = -\epsilon_0\chi(\nabla\psi(\mathbf{r})_{\mathbf{r}=\mathbf{r}_{\text{surf}}})\cdot\hat{n}, \tag{2}$$

where $\mathbf{r}_{\text{surf}}$ represents the location of the induced charge on the solute surface, $\hat{n}$ is the unit radial vector normal to the surface, $\mathbf{P}(r)$ is the polarization, and $\chi=\epsilon_{\text{in}}/\epsilon_{\text{out}}-1$, which represents the ratio of the electric permittivity of the solute to that of the surrounding media. Since we treat the solvent explicitly, we set $\epsilon_{\text{out}}=1$. For the cylindrical geometry investigated here, one can derive an explicit expression for the induced charge,[24]

$$\sigma_{\text{ind}}(R_c,\phi,z) = \sum_{m=-\infty}^{\infty} e^{im\phi}\int_0^{\infty} dk \frac{(\kappa-1)q}{2\pi^2 R_c} \times \frac{I'(kR_c)K_m(kd)}{I_m(kR_c)K'_m(kR_c)-\kappa I'_m(kR_c)K_m(kR_c)}\cos(kz), \tag{3}$$

where $\kappa=1+\chi$, R_c is the location of induced charges inside the cylinder, and d is the distance to an external point charge q. The solute polarizability is manifested in the simulations by computing at each time step the induced charge on the surface of the dielectric due to the charge distribution of the water molecules. Following our previous work, the induced charges are implemented by considering a grid of point charges that envelops the cylindrical surface.[24] The magnitude of the charge for each grid point is determined by Eq. (3). The solute-solute interactions were handled through the induced charge method described above. For a given solute we compute the induced charge due to the external charges. The induced charge configuration on one solute is then used to compute the induced charge on another solute, and the process is iterated through convergence.

In order to prevent the collapse of the external charges on the induced charges, we consider a repulsive potential $(\sigma/r)^n$, where $\sigma=9$ Å and $n=50$ for our simulations, which allows for a 1 Å penetration of water molecules with k_BT thermal energy. In all simulations, the dielectric discontinuity is set at $R_c=7$ Å. We emphasize that the only source of attractive interactions between the solute and the solvent is that due to the polarization of the solute by the solvent. Hence, our model can be used to investigate systematically the effect of solute polarizability on hydrophobicity just by changing the ratio $\epsilon_{\text{in}}/\epsilon_{\text{out}}$ in Eq. (3). For $\epsilon_{\text{in}}=1$ the solvent-solute interaction is completely repulsive and we recover a perfectly hydrophobic object. The computer simulations were performed within the *NVT* ensemble at $T=298$ K, using the Nosé-Hoover thermostat and a time step of 0.002 ps. The number of water molecules was varied from run to run (2000–4000) in order to ensure that the total pressure in the system was approximately zero (±0.1 kbar). The forces were computed over trajectories >1.2 ns.

The computation of the cylinder-water contact angles, described below, were performed with a slab of 3284 water molecules with an interfacial area of 80×80 Å^2. The simulations were performed again in the canonical ensemble (*NVT*) at 298 K, using a time step of 0.002 ps. The electrostatic interactions were computed using the three dimensional version of the Ewald summation method. This method has been shown to be accurate in the simulation of elongated molecules such as DNA.[30] A cutoff of 14 Å was set for the short-range non-Coulombic interactions. A typical simulation consisted of 0.5 ns equilibration and 1 ns production.

III. RESULTS

We first quantify the hydrophobicity of our polarizable objects through the evaluation of the solute-water contact angle. To this end we consider a geometric construction,[31] in which the cylindrical solute is sitting at the water-vapor in-

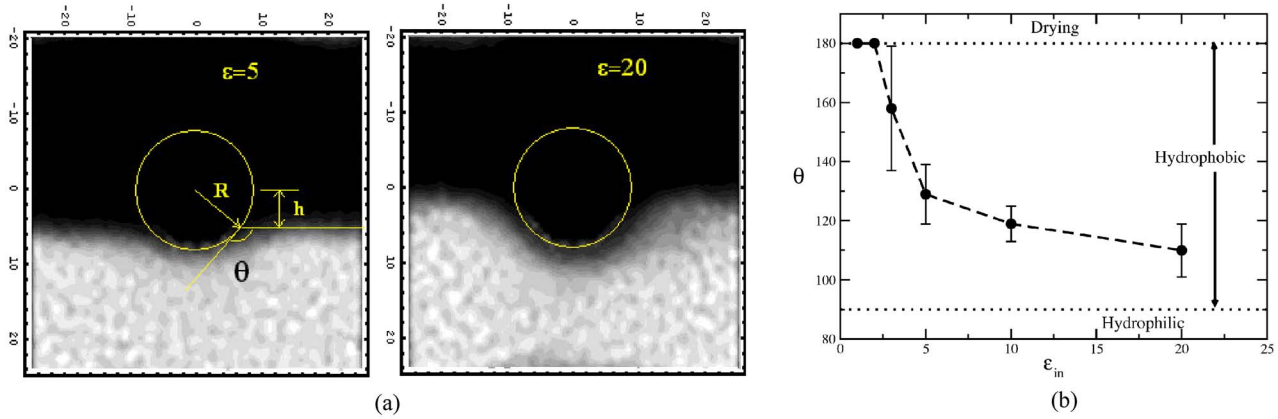

FIG. 1. (a) Average density profiles of the water-vapor interface around polarizable cylindrical solutes (cross-sectional view). Light colors indicate high density, dark, low density. Definitions of the geometrical variables needed to compute the contact angle, $\cos\theta=-h/R$, are given in the figure. (b) Dependence of the contact angles with solute polarizability.

terface [see Fig. 1(a)]. Our results for purely hydrophobic objects, $\epsilon_{in}=1$, and very weakly polarizable objects, $\epsilon_{in}=2$, indicate that these solutes exhibit complete drying, $\theta=180°$ [see Fig. 1(b)]. Nonetheless, a small increase in the polarizability, $\epsilon_{in}\geqslant 3$, is enough to induce partial wetting. The contact angles vary the greatest over the small interval of permittivities, $\epsilon_{in}=1-10$, a range that is relevant to biological systems, and varies more slowly for highly polarizable objects, $\epsilon_{in}\geqslant 10-20$. This contact angle behavior derives from the induced charges' dependence on solute polarizability, which scale approximately with the dielectric permittivities as[32] $(\epsilon_{in}-\epsilon_{out})/(\epsilon_{in}+\epsilon_{out})$, demonstrating that the rapid variation of the contact angles occurs over the same interval as large variations of the induced charges. Our results for highly polarizable objects, $\epsilon_{in}\geqslant 10-20$, indicate that the solutes are, strictly speaking, hydrophobic ($\theta>90°$). There are a number of real substances (e.g., GaAs semiconductors) that are highly polarizable ($\epsilon>11$) and hydrophobic ($\theta\approx 110°$).[33] Nonetheless, we would like to point out that there is no trivial relationship between polarizability and contact angle when comparing different materials. One can find hydrophilic materials with a moderate dielectric constant (e.g., for silicon dioxide, $\epsilon>4.5$). Thus, a direct comparison between different materials is not possible in terms of their polarizability alone. In the present study, however, we can isolate the polarizability contribution, since within our model the only difference between the solutes is their permittivities.

In order to understand the influence of the polarizability on the magnitude of the hydrophobic force and the hydrophobic interaction mechanism, we have investigated the force between two identical polarizable objects in water. As described above, the simulations consisted of two solutes with dielectric constant ϵ_{in}, separated by an interaxial distance D, which are immersed in water. Figure 2(a) shows the variation of the solute-solute force as a function of the separation D and solute polarizability. Our results show that the force is strongly dependent on the permittivity (polarization) of the solute. Only weakly polarizable objects $\epsilon_{in}\sim 1-3$ can sustain a vapor cavity (drying) at distances larger than contact, $D=17$ Å, resulting in a force that is effectively constant with solute separation.

The behavior of purely hydrophobic objects can be explained using a simple thermodynamic model that considers the balance of the free energies of two states; one in which there is a vapor cavity (dry state), Ω_v, and another one in which the cavity is filled with water, Ω_l,[34]

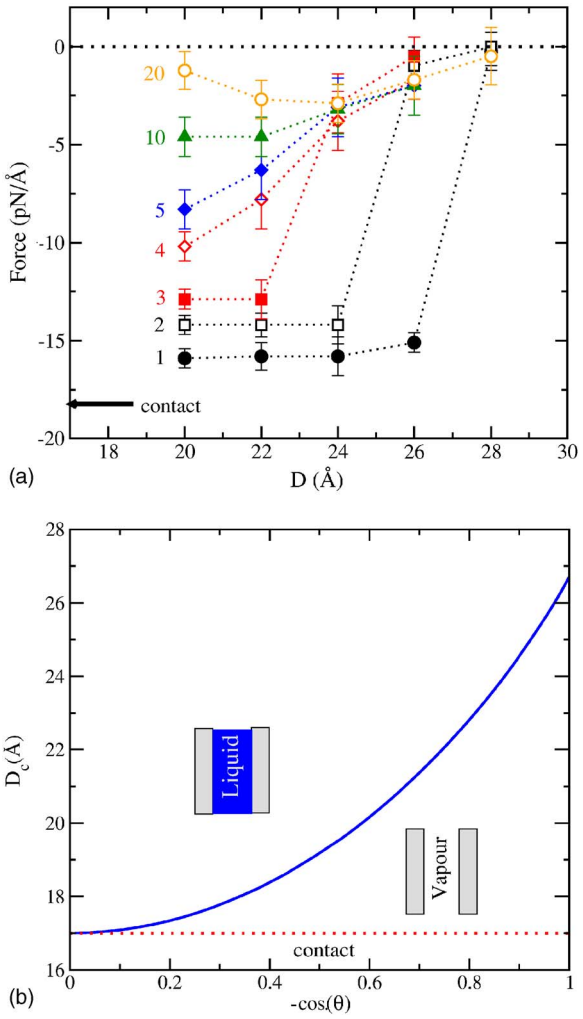

FIG. 2. (a) Variation of the intersolute force with solute-solute separation D for solutes with different polarizabilities. (b) The critical distance D_c (interaxial separation) for cavity stability between the two cylinders as a function of the contact angle θ obtained from Eq. (1).

$$\frac{\Delta\Omega}{l\gamma_{lv}} = \frac{\Omega_{lv} - \Omega_l}{l\gamma_{lv}} = \frac{(P - P_v)A}{\gamma_{lv}} + 2L_{cv}\cos(\theta) + 2L_{lv} + 4\frac{\tau}{\gamma_{lv}}, \tag{4}$$

where $\cos(\theta) = (\gamma_{sv} - \gamma_{sl})/\gamma_{lv}$ is the water-solute contact angle; $\gamma_{\alpha\beta}$ are the surface tensions of the liquid-vapor (lv), solute-liquid (sl), and solute-vapor (sv) interfaces; τ is the line tension; A is the cross-sectional area of the cavity; L_{cv} and L_{lv} are the lengths of the solute-vapor and liquid-vapor interfaces in the plane perpendicular to the cylinders' axes, respectively; and l is the length of the cylindrical solute, 34 Å in this work. The line tension term does not contribute to the force between the solutes, since in our model the length l does not vary with the intersolute separation. In general we expect that this contribution will not be very important since the line tension is typically of the order of $\tau \approx 10^{-12}-10^{-10}$ N.[31,35] Equation (4) predicts a discontinuity in the force at a specific separation D_c where a drying transition occurs. This is in agreement with our results for weakly polarizable objects, $\epsilon_{in}=1-3$ [see Fig. 2(a)]. The thermodynamic model also predicts that an increase in the polarizability (reduction in the contact angle θ) destabilizes the vapor cavity, shifting the solute-solute separation for drying to smaller distances [cf. Fig. 2(b)]. Considering the water molecule diameter (3 Å) and the solute diameter (17 Å), the shortest intersolute distance for which one could observe a cavity due *only* to drying is ≈20 Å, which corresponds to a contact angle ≈125° [Fig. 2(b)]. Combining this with the simulation data for contact angles [Fig. 1(b)], the theory suggests that the drying transition should not be observed for $\epsilon_{in} \geqslant 4-5$. This is consistent with our simulation results for the intersolute force [Fig. 2(a)]: no discontinuities exist for $\epsilon_{in} \geqslant 4$. Nonetheless the forces for these ϵ_{in} values decrease monotonically with intersolute distance and at short intersolute separations, they are of an order of magnitude similar to that of the forces due to drying. This observation cannot be explained with the thermodynamic model. According to this model for separations above the critical one, D_c, there should be bulk water in the interstitial regions between the solutes, and accordingly the solute-solute force should be zero. Then, what is the origin of the observed strong attractive forces?

To understand the origin of intersolute forces, we have investigated the density of water in the interstitial region between the two solutes. The density was obtained by computing the average number of water molecules in the center of the interstitial region defined by a prismatic volume with dimensions $4\times4\times34$ Å^3, centered at the plane that bisects the two-cylinder system. The existence of drying transitions for weakly polarizable objects ($\epsilon_{in} \leqslant 3$) is reflected in the interstitial densities, which feature a discontinuous jump, from low density to high density states [see Fig. 3(a)], at the same separations where the force showed a discontinuity [see Fig. 2(a)]. For higher polarizabilities ($\epsilon_{in} > 4$) we find that the density increases monotonically and lies always in between the bulk vapor and bulk liquid densities [cf. Fig. 3(a)]. Again, this observation is not consistent with the thermodynamic model, where only densities corresponding to the vapor or liquid are expected [cf. Eq. (4)]. One possible explanation of our results could be that the low density phase is actually an average over the liquid and the vapor states. This would engender that energy barriers between the two states in the interstitial region would have to be of the order or less than k_BT. We have investigated the possibility of having intermittent liquid-vapor states by computing a histogram that shows the water density fluctuations in the interstitial region. For a two state (liquid-vapor) model the histogram should conform to a bimodal distribution, yet we observe a single maximum with significant fluctuations conforming to a Gaussian distribution [see Fig. 3(b)]. Another possible explanation for the low densities could be the formation of liquid-vapor interfaces inside the cavity, but we do not find evidence for the development of well defined interfaces (see below). Finally, we find that the low density states reported above are reproducible and independent of initial conditions. Simulations commencing with the two extreme conditions [(1) a cavity is assumed in the interstitial region and (2) the interstitial region is full of water at bulk density] reveal that after a transient regime of about 0.2 ns, the interstitial densities for both cases converge to the same average [cf. Fig. 3(c)]. Moreover, the density fluctuation distributions associated with the final states for both systems match [cf. Fig. 3(b)].

These analyses demonstrate the stability of the low density states and their lack of dependence on the initial configuration of the system and also indicate that the low density phases correspond to minimum free energy states. As a further proof of this, a link can be made with recent work on carbon nanotubes.[36] For this system, water can develop densities inside a nanotube which are higher than the bulk water density. The excess chemical potential difference for a water molecule to be inside the nanotube as compared to being in the bulk was calculated to be $\approx -1.5k_BT$ (favoring filling of the tube), in good agreement with the excess chemical potential obtained from the water density inside the nanotube and in bulk, i.e., $\mu_{in}^{ex} - \mu_{bulk}^{ex} = -k_BT \ln[\rho_{in}/\rho_{bulk}]$. With regard to the two-cylinder system described above ($D=24$ Å, $\epsilon_{in}=5$, $\rho_{in}=0.4$), a similar argument reveals an excess chemical potential for a water molecule in the interstitial region as compared to being in bulk of $\mu_{in}^{ex} - \mu_{bulk}^{ex} = -k_BT \ln[\rho_{in}/\rho_{bulk}] = +0.9k_BT$, within the range of the thermal energy, thus demonstrating the important role thermal fluctuations play in these confined systems.

These thermal fluctuations can be directly observed in the simulations. Additional simulations were performed to investigate the formation of liquid-vapor interfaces or alternating liquid and vapor states in between the two polarizable solutes. We computed the water density in the interstitial region, between the two solutes, as a function of the position in the interstitial region (see Fig. 4) and the time, $\rho(z,t)$. This density profile can be used to analyze the existence of enduring liquid-vapor interfaces and/or liquid and vapor phases forming in the confined region. The analysis was performed over 120 ps. The results are represented in Fig. 4 as a two dimensional projection of the profile. The picture that emerges from this analysis is that the confined region is characterized by inhomogeneous regions consisting of water clusters. These regions evolve very rapidly with time resulting in the fluctuations discussed in Fig. 2(b). Our results do

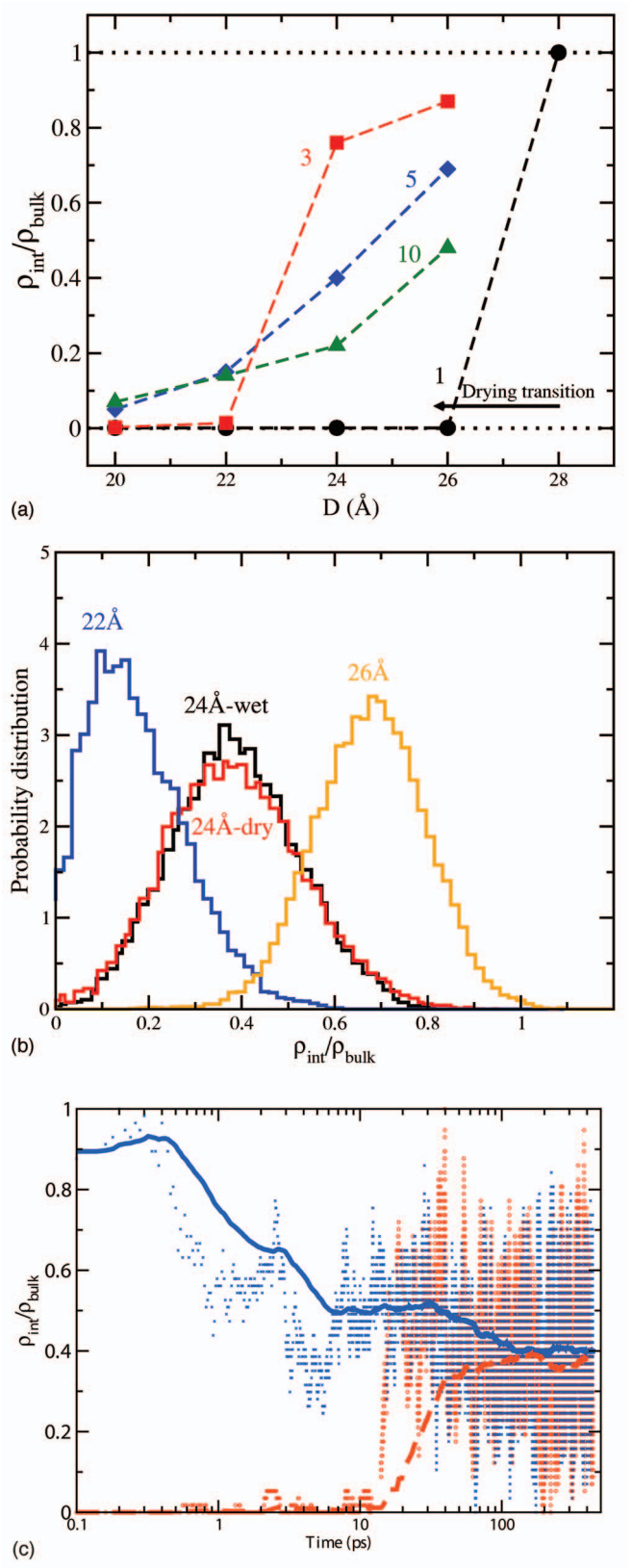

FIG. 3. (Color) (a) Variation of the interstitial water density with solute-solute separation for various dielectric permittivities. (b) Probability distribution of a given water density in the interstitial region for a representative system, $\epsilon_{in}=5$. For $D=24$ Å, the distributions corresponding to two systems starting from different initial conditions, dry and wet, are depicted (see text for details). (c) Variation of the interstitial density over time for $\epsilon_{in}=5$ and $D=24$ Å, for two different initial conditions, dry and wet. The symbols represent the densities at a specific time (stars, wet: circles, dry), whereas the lines correspond to the running time average (full line, wet; dashed line, dry).

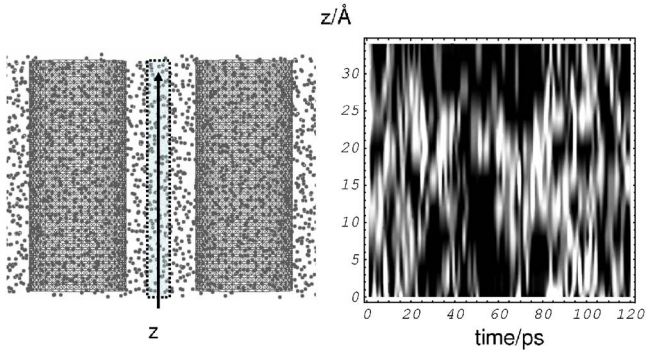

FIG. 4. Two dimensional projection of the time dependent density profile along the interstitial region between the two polarizable solutes (right). The results are shown for a representative system ($D=24$ Å, $\epsilon_{in}=5$). Zero density regions are represented in black and high density regions (bulk liquid, 1 g/cm^3) in white. The interstitial density profile was computed using a prismatic volume of dimensions $4\times4\times34$ Å^3 with a bin size of 3 Å along the z axis. See highlighted region in the snapshot depicted on the left (dark circles represent the oxygen atoms in the water molecules).

not show evidence for the existence of well defined liquid-vapor interfaces. Also, the density profile does not conform to the idea of a confined region consisting of intermittent liquid and vapor phases.

In view of the discussions above, the forces reported in Fig. 2(a) arise out of equilibrium states. We can conclude then that polarization has a dramatic effect on the intersolute forces. Indeed, there is nearly a direct correlation between the interstitial water densities of these equilibrium states and the forces between the cylinders. At small solute separations, lower dielectric solutes may support cavities, but with increasing polarization, there is an increase in the interstitial water density and, hence, a reduction of the intersolute force. At larger separations, however, solutes with larger polarizabilities interact to a greater degree with the solvent, leading to greater ordering, and thus, lower density of the solvent near the solutes (see, for instance, Figs. 2 and 3 in Ref. 24). This is also manifested in the crossover in the forces observed in Fig. 2(a), where forces between solutes with larger polarizabilities are observed to be longer ranged than those for smaller polarizabilities. Nevertheless, over the range of polarizabilities studied here, and whether there is drying or not, these forces are quite significant. Considering a hydrophobic unit of length 1 nm, which is approximately the size of amino acids in solution, one finds that at $D=20$ Å, which is close to contact, the attractive forces vary in magnitude from $\approx$100 pN ($\epsilon_{in}=1$) down to $\approx$10 pN ($\epsilon_{in}=20$). At intermediate polarizations [see $\epsilon_{in}=4,5$ in Fig. 2(a)], the forces associated with the low density states are at small intersolute distances of the same order of magnitude as the forces associated with drying, $\approx$75 pN.

IV. SUMMARY AND FURTHER REMARKS

We have investigated the influence of solute polarizability on the interactions between hydrophobic solutes in water. The polarizability is found to have a strong influence on the solute hydrophobicity (water contact angle) with the largest variations in the interval $\epsilon_{in}=1-10$. With respect to interactions between polarizable solutes, we find that capillary drying is inhibited for $\epsilon_{in}\sim4-5$, suggesting that drying transi-

tions would appear only under rather exceptional circumstances, i.e., for extremely hydrophobic objects ($\theta \approx 180°$). At short intersolute distances the forces between weakly polarizable objects are nonetheless of the same order of magnitude as the capillary forces associated with drying. The microscopic origin is quite different, however, and arises from the stabilization of water states with densities that lie in between that of vapor and liquid water, between the polarizable objects. This observation is not consistent with a two state thermodynamic model that defines the interstitial region between the solutes as a cavity where *only* liquid or vapor can exist. Thermal fluctuations, coupled with interactions of water molecules with the polarizable media, may disallow the formation of stable interfaces between the liquid-vapor states. Our results suggest that drying might not be the main mechanism operating in the self-assembly of hydrophobic surfaces.

ACKNOWLEDGMENTS

The authors would like to thank the EPSRC (F.B.) and The Royal Society (A.W.) for financial support. One of the authors (F.B.) would like to thank Professor Dietrich and Dr. Oettel for their hospitality at the Max Planck Institute for Metal Research-Stuttgart, where this manuscript was completed. Computer resources on HPCx was provided via the UK's HPC Materials Chemistry Consortium (EPSRC Grant No. EP/D504872). The authors would like to acknowledge the Barcelona Supercomputer Center (Spain) for providing resources on the Mare Nostrum Supercomputer, and the London eScience Centre at Imperial College London (UK) for resources in the Viking Cluster.

[1] J. Israelachvili, *Intermolecular and Surface Forces*, 2nd ed. (Academic, New York, 1991).
[2] W. Kauzmann, Adv. Protein Chem. **14**, 1 (1959); C. Tanfort, Science **200**, 1012 (1978).
[3] L. F. Scatena, M. G. Brown, and G. L. Richmond, Science **292**, 908 (2001).
[4] S. M. Pal, J. Peon, and A. H. Zewail, Proc. Natl. Acad. Sci. U.S.A. **99**, 1763 (2002).
[5] F. H. Stillinger, J. Solution Chem. **2**, 141 (1973).
[6] K. A. Sharp, A. Nicholls, R. F. Fine, and B. Honig, Science **252**, 106 (1991); N. T. Southall and K. A. Dill, J. Phys. Chem. B **104**, 1326 (2000).
[7] K. P. Murphy, Biophys. Chem. **51**, 311 (1994).
[8] R. L. Baldwin, Proc. Natl. Acad. Sci. U.S.A. **83**, 8069 (1986).
[9] R. M. Pashley, P. M. McGuiggan, B. W. Ninham, and D. Fennell Evans, Science **229**, 1088 (1985); H. K. Christenson and P. M. Claesson, *ibid.* **239**, 390 (1988); J. L. Parker, P. M. Claesson, and P. Attard, J. Phys. Chem. **98**, 8468 (1994).
[10] K. Lum, D. Chandler, and J. D. Weeks, J. Phys. Chem. B **103**, 4570 (1999).
[11] H. K. Christenson and P. M. Claesson, Adv. Colloid Interface Sci. **91**, 391 (2001).
[12] K. Leung, A. Luzar, and D. Bratko, Phys. Rev. Lett. **90**, 065502 (2003).
[13] N. Choudhury and B. M. Pettitt, J. Am. Chem. Soc. **127**, 3556 (2005).
[14] N. Giovambattista, P. J. Rossky, and P. G. Debenedetti, Phys. Rev. E **73**, 041604 (2006).
[15] D. A. Doshi, E. B. Watkins, J. N. Israelachvili, and J. Majewski, Proc. Natl. Acad. Sci. U.S.A. **102**, 9458 (2005).
[16] J. A. Ernst, R. T. Clubb, H. X. Zhou, A. N. Gronenborn, and G. M. Clore, Science **267**, 1813 (1995).
[17] R. Zhou, X. Huang, C. J. Margulis, and B. J. Berne, Science **305**, 1605 (2004).
[18] M. S. Cheung, A. E. García, and J. N. Onuchic, Proc. Natl. Acad. Sci. U.S.A. **99**, 685 (2002).
[19] P. Liu, X. Huang, R. Zhou, and B. J. Berne, Nature (London) **437**, 159 (2005).
[20] G. King, F. S. Lee, and A. Warshel, J. Chem. Phys. **95**, 4366 (1991).
[21] R. Allen, S. Melchionna, and J. P. Hansen, Phys. Rev. Lett. **89**, 175502 (2002).
[22] A. Parsegian, Nature (London) **221**, 844 (1969).
[23] A. A. Kornyshev and S. Leikin, J. Chem. Phys. **107**, 3656 (1997).
[24] A. Wynveen and F. Bresme, J. Chem. Phys. **124**, 104502 (2006).
[25] H. J. C. Berendsen, J. R. Grigera, and T. P. Straatsma, J. Phys. Chem. **91**, 6269 (1987).
[26] P. G. Kusalik and I. M. Svishchev, Science **265**, 1219 (1994).
[27] A. Wallqvist, Chem. Phys. Lett. **165**, 437 (1990).
[28] A. Kohlmeyer, W. Witschel, and E. Spohr, Chem. Phys. **213**, 211 (1996).
[29] J. D. Jackson, *Classical Electrodynamics*, 3rd ed. (Wiley, New York, 1999).
[30] J. Norberg and L. Nilsson, Biophys. J. **79**, 1537 (2000).
[31] F. Bresme and N. Quirke, Phys. Rev. Lett. **80**, 3791 (1997).
[32] L. D. Landau, E. M. Lifshitz, and L. P. Pitaevskii, *Electrodynamics of Continous Media*, 2nd ed. (Butterworth-Heinemann, Oxford, 1984).
[33] K. Autumn, M. Sitti, Y. C. A. Liang, A. M. Peattie, W. R. Hansen, S. Sponberg, T. W. Kenny, R. Fearing, J. N. Israelachvili, and R. J. Full, Proc. Natl. Acad. Sci. U.S.A. **99**, 12252 (2002).
[34] K. Lum and A. Luzar, Phys. Rev. E **56**, R6283 (1997).
[35] F. Bresme and N. Quirke, J. Chem. Phys. **110**, 3536 (1999).
[36] G. Hummer, J. C. Rasaiah, and J. P. Noworyta, Nature (London) **414**, 188 (2001).